José Ernesto Figueroa-García · Osvaldo Franco-Ramos · José María Bodoque · Juan Antonio Ballesteros-Cánovas · Lorenzo Vázquez-Selem

Long-term lahar reconstruction in Jamapa Gorge, Pico de Orizaba (Mexico) based on botanical evidence and numerical modelling

Abstract Lahars on volcanic terrain are recurrent phenomena with a high capacity to transform landscape and cause significant economic and life losses. Lahars have been studied in most volcanic regions, mostly based on the recognition of cotemporaneous events. Yet, there is a lack of long-term record about their frequency and magnitude. Such long-term records could help to improve lahar risk assessment and understand climate triggering factors. Here, we aim at providing the longest annual resolved frequency-magnitude lahar records of the Trans-Mexican Volcanic Belt. We focus on the Jamapa Gorge of the Pico de Orizaba volcano and apply geomorphological and dendrogeomorphological methodological approaches. Besides, we used a 2D numerical model to estimate the discharge of the reconstructed lahars based on the paleostage indicators (PSIs) defined by scars on trees. A total of 78 *Pinus hartwegii* trees were sampled for the reconstruction of lahars. We identified 157 growth disturbances related to past lahar activity, namely scars (51%), growth suppression (35%), and compression wood (32%). A total of 8 lahars were reconstructed between 1930 and 2017 (1931, 1960, 1968, 1975, 1999, 2012, 2014, and 2016) with a reconstructed peak discharge ranging between 80 and 350 m³/s. Largest events occurred in 1975 and 2012 with lahar discharges of 160 m³/s and 91 m³/s, respectively. Lahar events were linked to intense rainfall events and the passage of hurricanes and tropical storms coming from the Atlantic Ocean. These results highlight the benefit of the combined use of dendrogeomorphology and numerical modeling to gather longer series of lahar activity in volcanoes, where such information is largely lacking. The methodological approach deployed here can be applied consistently and uniformly in other volcanic regions to characterize lahar hazard, regardless of physiographic and climatic contexts.

Keywords Lahar · Dendrogeomorphology · Pico de Orizaba · Physically based flow model · Paleostage indicators

Introduction

Lahars are hydro-volcanic processes occurring on volcanic environments. During a lahar event, the transported materials are a mixture of rock, water, and mud that travel at high speed through the ravines of volcanoes (Pierson and Major 2014). These events have a high sediment carrying capacity, and their mobility is related to their proportion of water and sediment (Smith and Fritz 1989). Due to the difficulty to predict lahar events and the lack of territorial planning, they cause every year hundreds of fatalities around the world, as well as a large amount of damages in infrastructure, housing, and agriculture (Thouret et al. 2020), which may jeopardize vulnerable communities living in volcanic zones (UN 2015). The analysis and understanding of lahar dynamics are fundamental to implement disaster risk reduction (DRR) strategies (Chmutina et al. 2019).

Improving the resilience of people living in volcanic regions requires the elaboration of reliable hazard and risk laharic maps (Pierson et al. 2014). To this end, the use of physically based numerical models has become popular since the 1990s, e.g. LaharZ model (Schilling 2014); Titan 2D model (Williams et al. 2008); FLO2D (O'Brien et al. 1993); or RAMMS (Christen et al. 2012). In combination with field-based analyses, different numerical models have allowed to reconstruct recent lahar events and to understand potential impacts by taking in consideration the spatio-temporal variations of physical parameters (Davila et al. 2007; Iverson et al. 1998; Muñoz-Salinas et al. 2009; Williams et al. 2008; Worni et al. 2012). For instance, the LaharZ model was used to reconstruct the lahars events of Ruapehu and Taranaki volcanoes, New Zealand (Stevens et al. 2003); while the Titan 2D was used to develop a lahar hazard map of Merapi volcano, Indonesia (Charbonnier and Gertisser 2012). The hydraulic model FLO2D has been also used to report the magnitude and impact of massive lahar events on Nevado de Huila volcano, Colombia (Worni et al. 2012), as well as laharic activity on Ischia Island, Italy (Nocentini et al. 2015), while the one-phase numerical model RAMMS was used to simulate lahar-like events in Guatemala (Luna 2007), Chile (Bono and Amigo 2015), and Mexico (Franco-Ramos et al. 2020).

Although the use of numerical models has contributed to define flood zones and perform hazard and risk assessment (Pierson et al. 2014), their reliability highly depends on the existing information of the event for model calibration and uncertainty constrains. Thus, gathering evidence-based information from lahar events activity is a real challenge, often constrained to recent events (Thouret et al. 2020). An alternative to gather long-term baseline data on unrecorded lahar events is the use of trees as lahar's eyewitness (Bollschweiler et al. 2010). Trees growing along lahar channels and slopes of volcanoes are sensitive to such extreme events (Bollschweiler et al. 2010; Pierson et al. 2011), and its analyses allow to (i) precisely define the temporality (annual or seasonal) of past events and (ii) to determine the affected areas along the channels (Franco-Ramos et al. 2013). Thus, botanical-based lahar reconstruction can be used to determine the timing and possible triggers of extreme events, including those of hydro-meteorological, seismic, and volcanic nature (Franco-Ramos et al. 2016a, b). Besides, some botanical evidence such as scars on trees represents a paleostage indicator (PSI) of the flow thickness, which can be used to calibrate numerical models (Wilhelm et al. 2019) and indirectly estimate the lahar magnitude (Franco-Ramos et al. 2020). The application of dendrogeomorphological methods for the reconstruction of geomorphic events in volcanoes is in constant evolution (Bollschweiler et al. 2010; Franco-Ramos et al.

2020; Franco-Ramos et al. 2013; Garrote et al. 2018; Salaorni et al. 2017; Stoffel et al. 2011). However, long-term records of the magnitude and temporality of lahars remain scarce worldwide, as is the case for the Pico de Orizaba volcano.

In this study, we aim at providing the longest lahar magnitude reconstruction of the Trans-Mexican Volcanic Belt (TMVB) and as far as we know in the world. Specifically, we focused on a sector of Jamapa Gorge located on the northern slopes of Pico de Orizaba, one of the largest volcanic structures in North America. Analogue to other botanical evidence-based approaches in mountain torrents (Ballesteros Cánovas et al. 2011 Díez-Herrero et al. 2013a, b; Bodoque et al. 2015; Garrote et al. 2018; Tichavský et al. 2020), here we combine botanical evidence from *Pinus hartwegii* trees growing along the gorge and numerical model resolved in high-resolution digital terrain models (DTM) obtained by unmanned aircrafts vehicles (UAVs) (Fernández de Castro Martínez et al. 2018). Finally, we use the reconstructed lahar record to analyze the potential occurrence of lahars based on data from the closer meteorological stations (Servicio Meteorológico Nacional (SMN) 2008, 2012, 2016) and the hurricane record (National Oceanic and Atmospheric Administration (NOAA) 2019). The results are expected to improve our understanding on the potential magnitude of expected lahars triggered by climatic factors, and therefore to contribute to the implementation of reliable disaster risk reductions strategies in the region.

Study site

The Pico de Orizaba or Citlaltépetl volcano is located on the eastern sector of the TMVB, between the states of Puebla and Veracruz (Fig. 1A). It is a composite cone of andesitic composition with an elevation of 5675 m a.s.l., which places it as the highest volcanic structure in North America (Carrasco-Núñez 2000). The volcano is located on large Mesozoic carbonate sequences of the Sierra Madre Oriental system. Its eruptive history consists of numerous explosive events including Plinian eruptions, sector collapses, extensive pyroclastic flows, and lahars from the late Pleistocene to the early to mid-Holocene, with relatively minor activity in the last few millennia and last observed activity in the late 16th and late 17th centuries (Hoskuldsson and Robin 1993; Siebe et al. 1993; Carrasco-Núñez 2000). Currently, the Pico de Orizaba is considered an active volcano but experiencing a quiet state. Due to its size and geographic position, it represents a major orographic barrier that divides the semi-arid central highlands from the more humid coastal plain of the Gulf of Mexico.

Figure 8A shows the year of the reconstructed lahar, with the occurrence of the hurricane and the recorded precipitation at the closest meteorological station. The lahars seem to be associated with accumulated rainfall of > 230 mm over 3 to 5 days for events in 1999, 2012, and 2016. Yet, these rainfall thresholds seem to be much lower (<130 mm over 3–5 days) in other years, i.e. 1931, 1960, 1975, and 2014, probably reflecting the non-linearity lahar response to environmental and climatic factors. Figure 8 A suggests an increase in lahar formation, going from one or two low to medium intensity phenomena per decade to two in the last decade. Figure 8 B shows the paths of hurricanes formed in the Atlantic Ocean that impacted the coasts of the Gulf of Mexico in the years when there was evidence of lahar formation in Jamapa Gorge. In all cases, the Pico de Orizaba volcano was located in the area of influence of

high humidity of 160 km, as per defined by National Oceanic and Atmospheric Administration (NOAA) (2019). This figure also shows that four of the five hurricanes (1931, 1960, 2012, and 2016) come into direct contact with this area of influence. In the case of the 1975 event, the path of the phenomenon is farther away from the volcano; however, it is the only one that reached category 3, according to NOAA intensity scale.

The Jamapa Gorge basin is located between 18° 45′ and 19° 13′ N and 96° 17′ and 97° 16′ W, beginning at the base of the Jamapa glacier at ~4800 m a.s.l. (Fig. 1C). It has an area of about 3912 km², almost entirely within the state of Veracruz, with an important socioeconomic interest for people (Comisión Nacional del Agua (CONAGUA) 2014). Precipitation in the area ranges from 1200 to 1700 mm per year, with highest values from June to October, according to data from the Huatusco station (30342) (Servicio Meteorológico Nacional (SMN) 2008, 2012, 2016).

Since the late Quaternary, the generation of volcanoclastic flows (avalanches and lahars) is a recurrent phenomenon on the slopes and valleys of the Pico de Orizaba volcano (Fig. 1B). Hoskuldsson and Robin (1993) proposed the existence of four large avalanches responsible for the current volcano morphology. However, Carrasco-Núñez et al. (2006) suggested that only two major collapse events affected the ancestral buildings of the Torrecillas Cone and Espolón de Oro Cone, namely events related to the (i) Jamapa Avalanche Deposit and (ii) Tetelzingo Avalanche-Lahar Deposit (4660 ±100 and 4040 ±80 y.B.P) (Siebe et al. 1993) . In the southeastern sector of the volcano, along the Metlac River, there is evidence of several smaller debris avalanches (Carrasco-Núñez et al. 2006), while in the northnortheastern slope, along the Huitzilapan Gorge, there are deposits of a major lahar that took place in 1920 ("Huitzilapan lahar"), triggered as a compounded effect of an earthquake of 6.5 M_L followed by torrential rainfalls (Carrasco-Núñez et al. 2006). Recently, on 5 June 2003, a large debris flow (~peak discharge of 350 m³ s⁻¹) occurred on the southern slope of Pico de Orizaba after a torrential rainfall (Rodríguez et al. 2006).

Methods

Fieldwork

Two fundamental aspects were considered for the delimitation of the study site. The first one is associated with the morphological evidence of the lahars, i.e. lobes, levees, terraces, and the main channel (Fig. 2A). The second one refers to the presence of trees with record of some geomorphological disturbance related to the occurrence of these phenomena in order to obtain samples with dendrogeomorphological potential. Based on the above criteria and the observations made in the field, the selected sector is located in the middle portion of the gorge, from 3630 m a.s.l. to its lower limit at 3530 m a.s.l. It has an area of 0.10 km² and a length of 650 m (Fig. 2B).

The fieldwork consisted in (i) obtaining field measurements and topographic data and (ii) sampling botanical evidence of past lahar activity from affected trees. First, we carried out a photogrammetric survey to obtain the topographic information from the studied gorge based on UAV. We used the DJI's Phantom 4 and Mavic Pro drones, considering a flight's height of 100 m above the surface and pictures taken with an 80% lateral and transversal
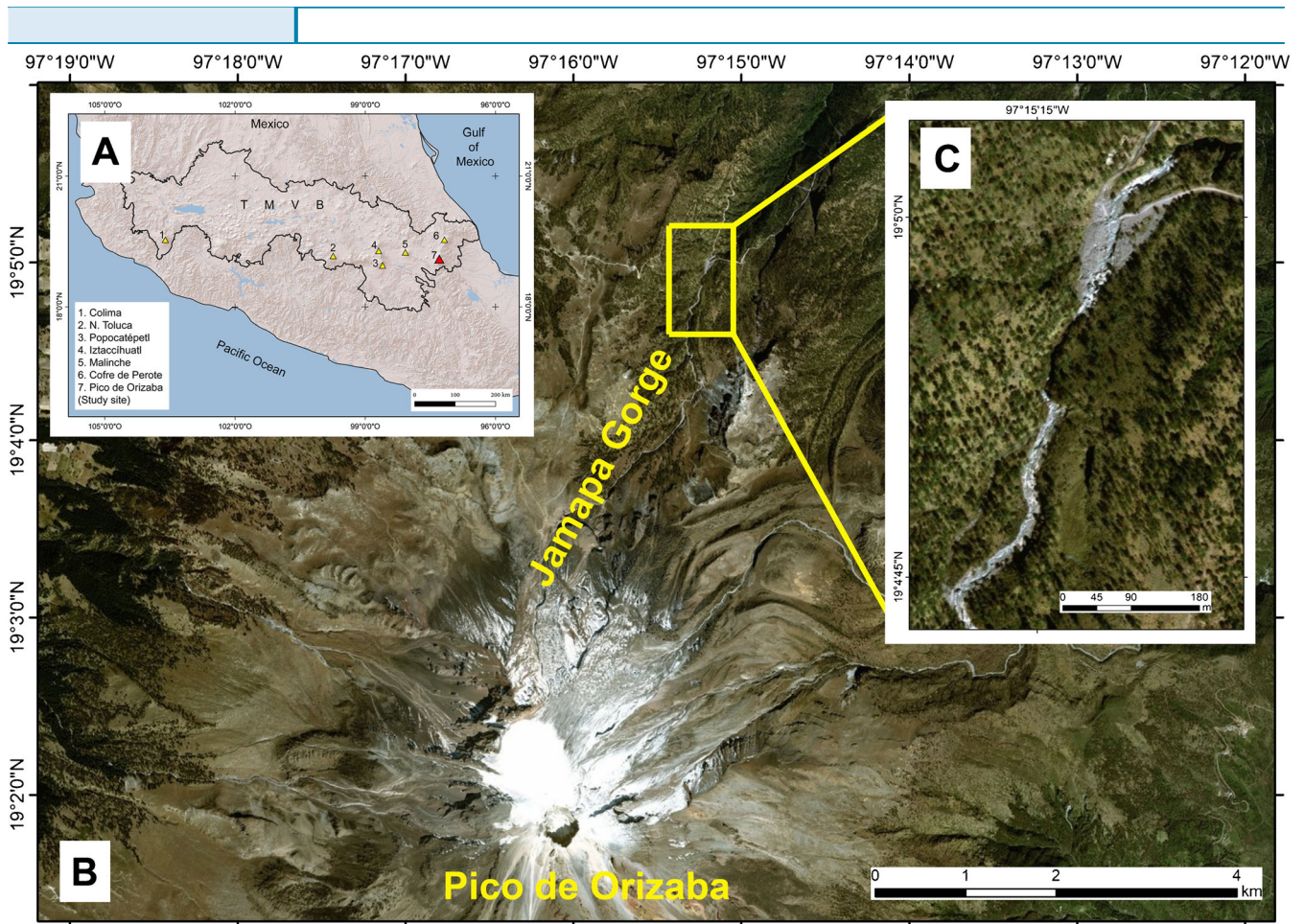
Fig. 1 A Location of Pico de Orizaba volcano in the Trans-Mexican Volcanic Belt. **B** and **C** Satellite image showing Pico de Orizaba and the location of the study area in Jamapa Gorge (Source Google Earth, 2019)

overlap (Fig. 3A). In the field, information about geomorphic features such as pyroclastic deposits, lava flows, and exogenous processes (i.e., laharic terraces, erosive landforms, and recent mass movement deposits) was recorded. Then, we recognized all the affected trees growing on each geomorphic feature related to lahar processes along the channel. To minimize the noise signal, only trees with clear evidence of damages by lahars were considered for sampling. These trees showed scars according to the flow direction at the basis of the stem and with sediments and clasts in the surroundings. We avoided elongated scars caused by fallen trees or lightning as well as scars with charcoal remains which may indicate fires processes. Sampling was done using *Pressler* drills and electric chainsaw to obtain 5 mm diameter cores and cross sections, respectively (Fig. 3B–C).
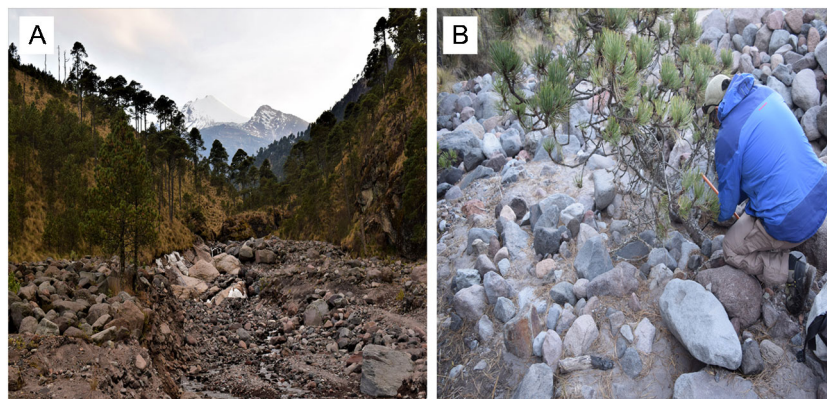
Fig. 2 A General view of the studied stretch of Jamapa Gorge showing the main channel filled by recent laharic deposits; a *Pinus hartwegii* forest covers the adjacent hillslopes and terraces. **B** Recent laharic deposits that have impacted the trees growing there
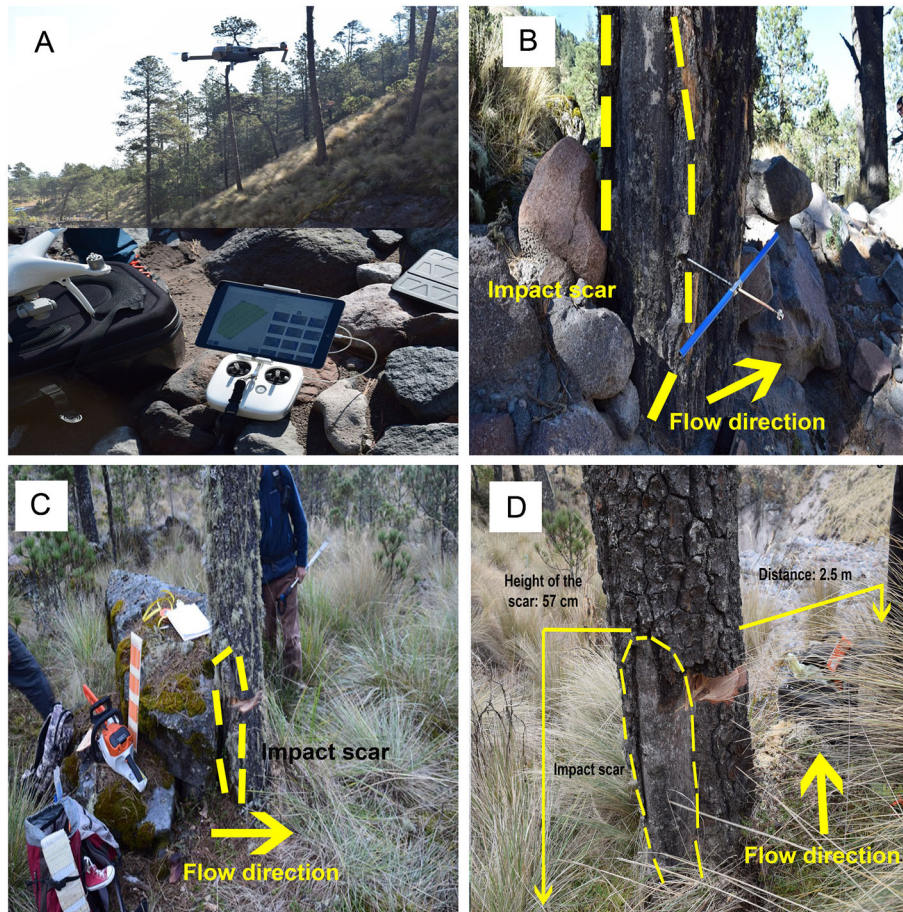
Fig. 3 **A** Launch of the UAV in the study site. **B** Increment cores collected using a *Pressler* drill, next to a lahar-derived scar, on terrace 5. **C** Tree killed by a lahar of year 1975 on terrace 3; a wedge sample was collected at 49 cm from the ground using a chainsaw. **D** Example of PSI and data collected for calibration of the models made in the RAMMS program

In total, we sampled 78 trees, obtaining 94 increment cores and 40 cross sections of the species *Pinus hartwegii*. In addition, we sampled 15 trees located in relatively stable and unaffected areas to build the reference chronology to recognize missing rings and determine growth disturbances in samples affected by geomorphological phenomena. In the field, additional information from trees such as the maximum height of the scar and their exact ground position was recorded (Ballesteros et al. 2011; Ballesteros-Cánovas et al. 2016). Figure 3 D shows some of the procedures to acquire field data. These were subsequently used in the calibration of the models generated in the RAMMS software, by means of a Geographic Information System (ArcGIS 10.5: ESRI 2016). To take the measurements described above, the sediment carrying capacity of lahars was considered, as they can transport all sizes of material, from ash to large boulders. Accordingly, it was assumed that the highest point of the impact scar in the sampled trees is equivalent to the flow thickness, thereby defining a PSI for estimating the peak flow of lahars (Ballesteros et al. 2011; Ballesteros-Cánovas et al. 2016).

Laboratory analysis

A total of 498 aerial images were processed in the PIX4DMapper software (Pix4D SA, Switzerland) in the following way: (1) loading and aligning the images; (2) generating and filtering the first point cloud; (3) densifying the point cloud; (4) classifying the ground points; (5) constructing the grid and smoothing the model; and (6) exporting the digital elevation model (DEM) and the orthomosaic (Fig. 4A). From the DEM, the orthomosaic, and fieldwork data, it was possible to make the geomorphological map of the gorge at a scale of 1: 1570. We used the classification of the morphogenetic features by Lugo-Hubp (1988). ArcGis 10.5 (ESRI 2016) software was used for their digital mapping.

All dendrogeomorphological samples were prepared according following Stokes and Smiley (1968). Once the samples were dated following standard procedures (Stoffel and Corona 2014), they were measured using a VELMEX (Robinson and Evans 1980) sliding plate connected to a computer and the TSAPWin™ software (Rinn 2003) (Fig. 4B). In this way, the precise width of each ring was obtained to generate the Tucson type file (.rwl), which is used in the COFECHA program (Holmes 1983), giving validity to the co-dating and the reference chronology. In addition, the disturbances identified in each of the samples were dated according to the criteria described by Stoffel and Corona (2014), who group them on the basis of the intensity and kind of reaction presented by the tree (Fig. 4C). When possible, the intra-position of injures within the annual increment growth (i.e., earlywood, latewood, or dormancy period) was used to distinguish the seasonality of the events (Stoffel and Corona 2014).
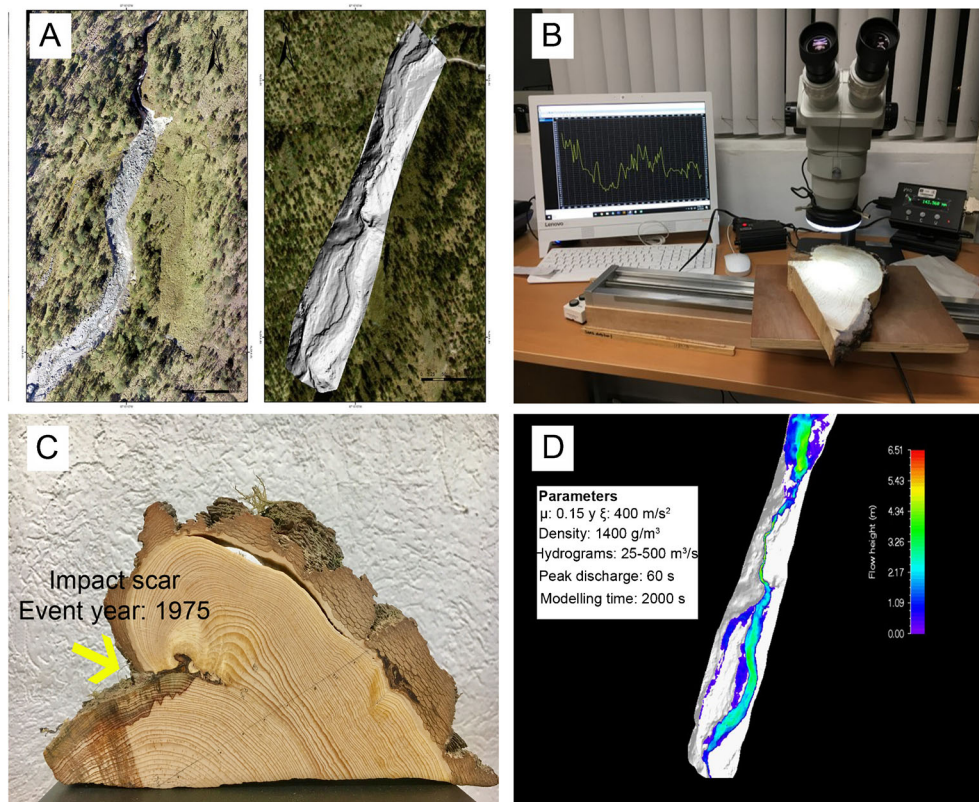
Fig. 4 **A** Orthomosaic and DEM obtained from UAV-images with 3.3 centimeters of resolution. **B** Dendrochronological workstation for measurement and analysis of tree-rings. **C** Example of a sample with evidence of scar in the year 1975. **D** Diagram and values of one of the flows modeled with RAMMS

Numerical modeling with RAMMS

Numerical modeling of laharic flows was performed using the one-phase RAMMS numerical model (WSL, Bühler et al. 2011; Christen et al. 2012; Fischer et al. 2012). This model uses the Voellmy-Salm fluid flow continuum model to simulate the runout of muddy and sediment-laden flows in mountain terrains (Iverson et al. 1998; Williams et al. 2008; Worni et al. 2012). In this model, the flow resistance is described by the Coulomb friction (μ), proportional to the normal stress at the flow bottom, and the viscous resistance turbulent friction (ξ-m/s^2), depending of the square of the maximum velocity. The model input data are (i) DEM, (ii) the initial discharge (volume or hydrograph), (iii) Coulomb friction (μ), (iv) turbulent friction (ξ), and (v) flow density (ρ). During the model setup, we

Table 1 Parameters used in RAMMS, and values used in the Jamapa Gorge

RAMMS Parameters Parameters	Values used in the Jamapa Gorge
Coulomb friction (μ)	0.15
Turbulent friction (ξ-m/s^2)	400
Density (g/m^3)	1400
Hydrographs (m^3/s)	25–500
Discharge peak (s)	60
Modeling time (s)	2000

used a 1-m resolution DEM derived by photogrammetry, while the assignment of initial friction values was obtained from the laharic events reported in other volcanoes in Mexico, such as the ones analyzed on Popocatepetl (Caballero and Capra 2014; Caballero et al. 2016) and Colima volcanoes (Capra et al. 2010). Accordingly, the values considered were μ= 0.15, which was defined on the basis of field observations and represents the average slope of the deposition zones (Voellmy 1955), and ξ= 400 m/s^2, which represents the nature of the flow observed in similar physiographic contexts in Mexico (Caballero and Capra 2014). The input discharge was added as hydrographs; in this sense, it was considered that in tropical environments, the discharge peaks in most of the ravines occur at 60 s, and for the modeling time, 2000 s were assigned, with the intention that the flow would cover the entire study area. Different peak discharges ranging from 25 to 500 m^3/s were modelled. The density considered for the flows was 1400 kg/m^3 (Table 1). A sensitive analysis was also carried out by varying ±25% friction and density parameters. Finally, the lahar magnitude assignment was based on the minimum average standard deviations between the water depth modelled and the maximum scar height dated for each event. Once these results were obtained, a linear regression was applied to them and the most adjusted input value was identified (Fig. 4D).

Hydrometeorological triggering of lahars

The reconstructed lahar activity (both occurrence and magnitude) was linked to rainfall data and in particular to the occurrence of
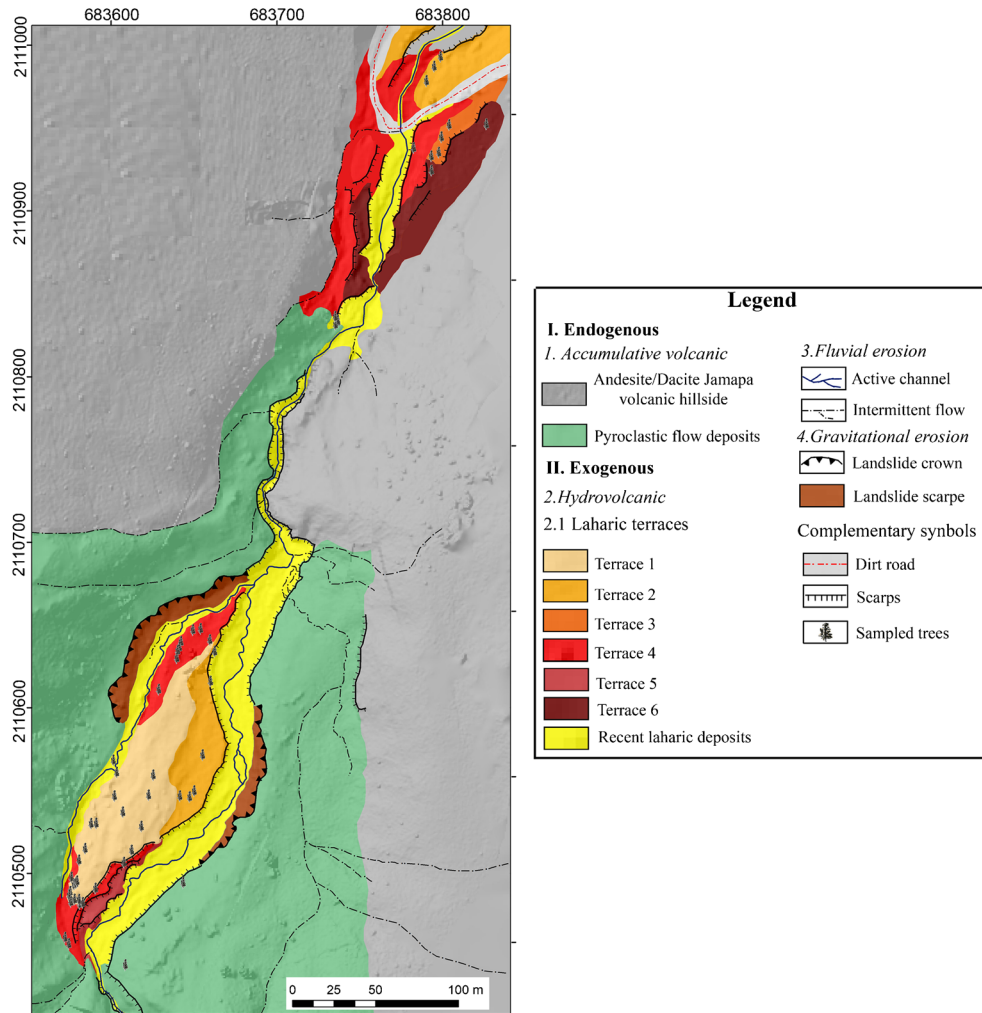
Fig. 5 Geomorphological map of Jamapa Gorge, Pico de Orizaba

extraordinary hydrometeorological phenomena. The linkages with rainfall events were possible due to the seasonal precision on the lahar reconstruction based on dendrogeomorphology. The analysis included data from meteorological stations near the study area (i.e., Coscomatepec; Ixhuatlán and Huatusco Station; Servicio Meteorológico Nacional (SMN) 2008, 2012, 2016). Owing to the lack of meteorological stations at the study site, we used the nearest available meteorological station, which is located 13 km away from the Jamapa gorge. In each database, we calculated the accumulated rainfall in 1, 3, and 5 days, considering the observations made by Capra et al. (2010) and Vàzquez et al. (2014) who associated the development of large volume debris flows with prolonged rainfall events linked to tropical storms or hurricanes. Usually these rainfall events release at least 20 mm h^{-1} of rain with a maximum intensity of 95 mm h^{-1} or even higher amounts reaching 400 mm during the 30 h with maximum intensities of 37 mm h^{-1} (Capra et al. 2018). Once these values were identified, we searched for the possible event that triggered the increase in rainfall, which mostly coincided with the occurrence of hurricanes from the Atlantic Ocean, so their paths were analyzed based on NOAA reports (2019).

Results

Dendrogeomorphic detection of lahar activity

The geomorphological analyses of the Jamapa Gorge reveal intense activity of exogenous processes shaping the pyroclastic deposits and lava flows associated with the andesites-dacites emplaced during the eruptive history of Pico de Orizaba. In the studied sector, six levels of laharic terraces and recent deposits were identified, modelled by fluvial and gravitational erosive processes (Fig. 5). Trees affected by recent lahar activity were growing on the latter geomorphic units, generally in the first and second laharic terraces, while unaffected trees used for the reference chronology were located in higher terrace levels, where the influence of fluvial and gravitational processes on trees was not observed. Samples from 15 *Pinus hartwegii* trees that did not show evidence of disturbances were used to build the reference chronology. The chronology covers the years 1709 to 2018. COFECHA indicated a significant correlation of 0.513 (P<0.01) with an average sensitivity of 0.291. Overall, 78 trees were sampled showing the average age of the samples trees was 74 years (n$_{obs}$=78). Disturbed trees allowed the identification of 157 growth disturbances, consisting of scars (51%), growth suppression (35%), and compression wood (32%).
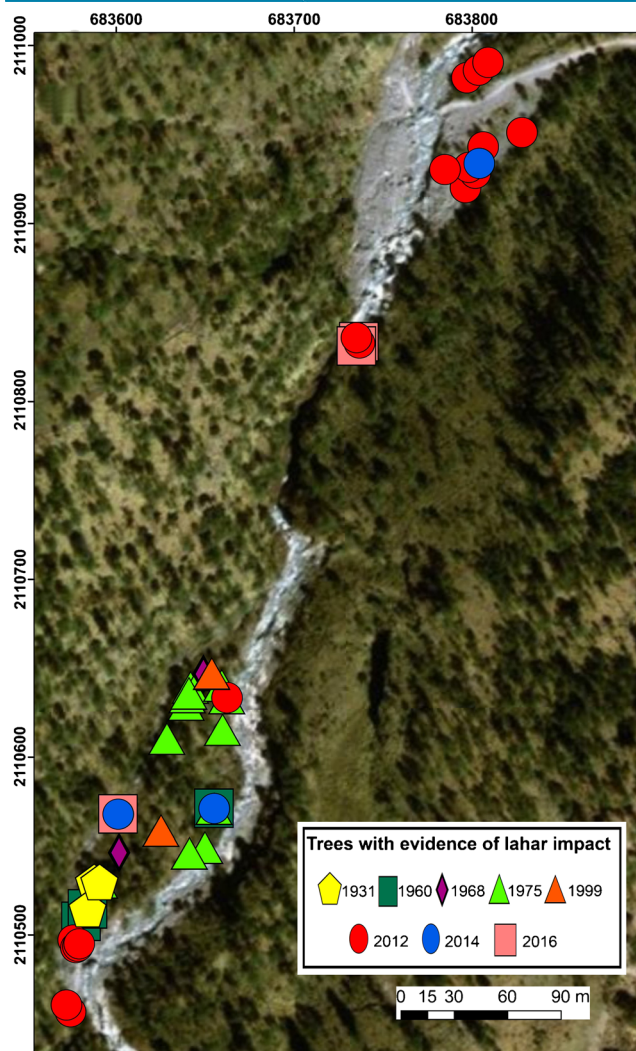
Fig. 6 Spatial distribution of tress showing tree-ring evidence of laharic events in the middle sector of Jamapa gorge

These growth anomalies lead to the detection of 8 lahars in the years 1931, 1960, 1968, 1975, 1999, 2012, 2014, and 2016. The lahars of 1975 and 2012 affected a large number of trees, 16 and 26 trees, respectively. Most of the trees with disturbances were in dynamic geomorphological positions such as low terraces and recent laharic deposits. Figure 6 shows the distribution of the trees which allowed the dating of the lahars.

Estimation of the lahar magnitude

The lahar magnitude estimation was based on 49 trees growing near the main channel and on low terraces. PSI defined by scars heights ranked from 0.032 to 1.35 m, with an average of 0.56 ± 0.32 m. Overall, the deviation between the flow modelled thickness and the height of scars for all reconstructed events ranked between −0.69 and 1.99 m, with an overall average of 0.004 ± 0.49 m (Fig. 7). The model parametrization we used was $\mu = 0.15$, $\xi = 400$ m/s^2, and flow density =1400 kg/m^3. The value that was modified for each case was the input discharge of the hydrograph. These and other results obtained are shown in Table 2. The average discharge reconstructed over the last century in the Pico de Orizaba was 174.5

± 82.5 m^3/s (n_{obs}=8). The largest lahar event took place in 2012, with a reconstructed magnitude of 91 m^3/s, while the smallest event took place in 2014, with a magnitude of 80 m^3/s. Based on the average deviation, the best adjustment between the PSI and modelled water depth was found for the lahar that took place in in 2012 (average deviation = −0.01m, n_{obs}=19, peak discharge = 91 m^3/s), while the event of year 1975 presented a less adjustment but not significant (average deviation = −0.04 m, n_{obs}=13, peak discharge =160 m^3/s).

### Hydrometeorological triggers of reconstructed lahars

Five out of eight reconstructed lahars were associated with extraordinary meteorological events such as the passage of hurricanes, namely hurricane "San Nicolas" in 1931, "Abby" in 1960, "Caroline" in 1975, "Ernesto" in 2012, and "Earl" in 2016. All these events occurred in the rain season of central Mexico, between July and October, which matches with the seasonality of the injuries observed in the tree-ring records. The other three events could not be linked to any extraordinary hydrometeorological event, because in the seasonal period in which the damage to the growth rings was detected, there is no record of any. However, they were associated with atypical precipitations that did coincide with the period.

Discussion and conclusions

We showed combined botanical and numerical model evidence supporting the longest lahar magnitude records of the TMVB. Our analyses revealed the occurrence of eight lahars since 1930, five of them (1931, 1960, 1975, 2012, and 2016) associated with the occurrence of hurricanes and the other 3 (1968, 1999, and 2014) associated with atypical rainfall (>100 mm accumulated over 3 to 5 days). The reconstructed lahar magnitude varied from 80 to 350 m^3/s, with larger events in 2012 (91 m^3/s) and 1975 (160 m^3/s). This information is highly relevant for DRR purposes, since data about the magnitude of lahars is uncommon in the region.

Dendrogeomorphological analyses using *Pinus hartwegii* have been conducted in other volcanoes of the TMVB (Bollschweiler et al. 2010; Franco-Ramos et al. 2017; Prado-Lallande 2017). *Pinus hartwegii* is one of the longest living species in Mexico (Villanueva-Díaz et al. 2010). Yet, the extreme, high elevation environments where this species grows make it very sensitive to disturbances that often cause changes in the growth and the formation of false rings (Villanueva-Díaz et al. 2010). Once these difficulties were identified and observed in the samples collected, it was possible to perform lahar reconstructions with precise dates. Our reconstruction is associated with some events recorded in other volcanoes of the central-east portion of the TMVB. In particular, Franco-Ramos et al. (2017) and Franco-Ramos et al. (2019) report rockfalls at Cofre de Perote and lahars in La Malinche in 1975. In the case of the 2012 event, laharic flows were also dated on Iztaccíhuatl (Prado-Lallande 2017), Popocatépetl (Franco-Ramos et al. 2016a), and La Malinche volcanoes (Franco-Ramos et al. 2019), apparently in connection with Hurricane Ernesto on the Gulf of Mexico coast on August 9, 2012 (National Oceanic and Atmospheric Administration (NOAA) 2019). These matches support the reliability of our reconstruction and suggest that lahar events respond to regional climate triggers.

Thus, the formation of lahars in Pico de Orizaba seems to be related to the occurrence of hurricanes, as previously reported in Popocatépetl (Bollschweiler et al. 2010; Franco-Ramos et al. 2016a),
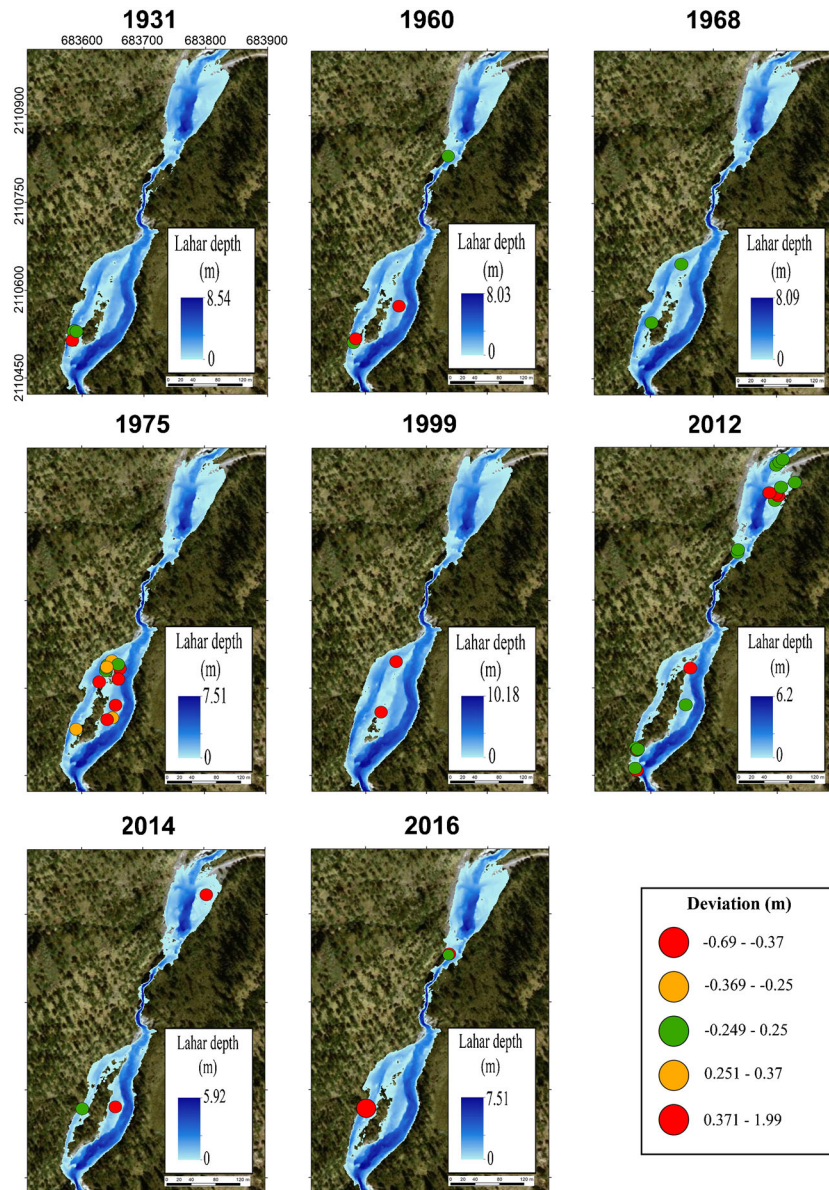
Fig. 7 Modeled depth of 8 laharic events based on tree-ring evidence. Circles show the standard deviation registered when comparing the height of the debarking and the depth value obtained from the simulation

La Malinche (Franco-Ramos et al. 2019; Franco-Ramos et al. 2016b), and Colima (Capra et al. 2010; Franco-Ramos et al. 2013), where the main trigger is a heavy rainfall (20–95 mm h⁻¹) accumulated over a period of no more than 5 days (200–400 mm), this sudden increase in rainfall being usually associated with hurricanes and tropical storms. Our results suggest that in Jamapa Gorge, lahars are linked to rainfall events exceeding 100 mm accumulated over 3 to 5 days. This rainfall threshold was reached in a single day probably associated with the lahar of 2016 (August 5, 2016; daily rainfall: 141 mm). Yet, we detected that in some events (i.e., 1931, 1960 and 2014), the contribution of rainfall (114–127 mm) was not as significant as in other years. Alternative reasons for the generation of debris flows are (1) fire on mountain slopes, which produces soil hydrophobicity and higher runoff leading to debris flows (Cannon and Reneau 2000; Staley et al. 2013); (2) the

increase in temperature in high mountain areas that favors glacier melting and the occurrence of sudden water inflows to mountain streams (Chiarle et al. 2007; Morales Martínez et al. 2016); and (3) the occurrence of regional climatic phenomena such as La Niña, which are characterized in central Mexico by atypical and intense rainfall (Franco-Ramos et al. 2016a, b; Vargas et al. 2006). It is possible that these three factors explain the formation of large and widely distributed lahars that are not associated with a hurricane. However, these linkages remain unclear and more evidence is needed to corroborate them.

We applied 2D numerical modeling to reconstruct the magnitude of lahars based on dendrogeomorphological evidences (Baker 2008; Ballesteros Cánovas et al. 2011 a,b; Benito and Thorndycraft 2005; Díez-Herrero et al. 2013a, b). For each event, a map was obtained in which its spatial distribution, the maximum flow rate,
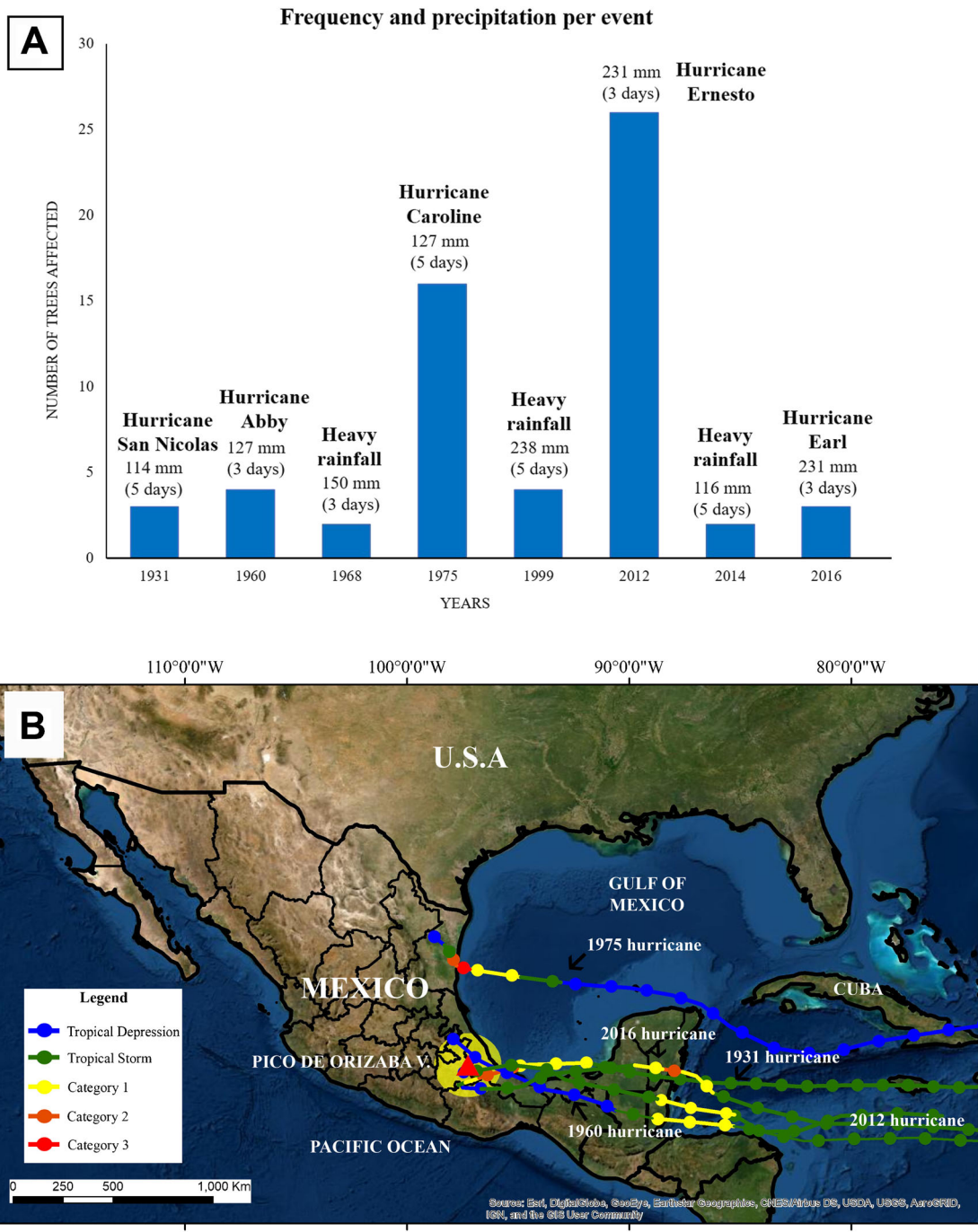
Fig. 8 **A** Relationship between identified lahars and rainfall data, as well as the possible associated hydrometeorological phenomenon. **B** Path of the hurricanes that were associated with the lahars identified in the study area

and the position of each collected tree were represented, as well as the standard deviation between the height of the debarking and the recreated flow rate value. The maximum depths recreated range from 5 to 11 m. However, it is necessary to be careful in the interpretation of these results, because in some events, the calibration based on PSI of trees shows a wide standard deviation between the debarking and the flow depth, as in the case of the lahars of 1931 (± −0.03) and 1975 (± −0.04). The opposite occurs for 1960 and 2012, when the modeled depth adjusts more precisely to most scars (±−0.01). Although we carefully chose the reach river

in term of bedrock, we recognize that the bars located in the upper and lower part of the studied area could be affected by geomorphic changes. These changes may partially explain the variation in the standard deviation, though other factors such the location of trees within the studied reach may affect (Ballesteros-Cánovas et al. 2016; Quesada-Román et al. 2020). We observed that trees located in areas close to the main channel, on the secondary channel, and on low terraces work as a better markers for calibration, while trees located on higher surfaces (stable terraces) or far from the points where the flow probably crosses show a higher deviation.

Table 2 Results of the 8 lahar events simulated with RAMMS and PSI calibration

Event year	Trees considered	Minimum and maximum deviation (m)	Average deviation (m)	Discharge (m³/s)	Maximum flow height (m)	Maximum flow rate (m/s²)
1931	3	0.13 to −0.39	−0.03	198	8.54	12.45
1960	4	−0.01–0.86	−0.01	176	8.03	18.26
1968	2	−0.03	−0.03	181	8.09	17.89
1975	13	−0.12–0.89	−0.04	160	7.51	18.37
1999	2	−0.38–0.42	0.02	350	10.18	16.11
2012	19	−0.01–1.99	−0.01	91	6.2	19.12
2014	3	0.1 to −0.59	−0.02	80	5.92	18.5
2016	3	−0.16 to −0.64	0.03	160	7.51	18.37

Similarly, another factor that can influence the calibration is the number of trees used. However, this fact was not considered a determining parameter for the interpretation of the results, because there are no elements to assess this issue. The average input discharge was 174.5 m³/s, with a minimum of 80 m³/s and a maximum of 350 m³/s. The peak discharge was set at 60 s and the software modeled 2000 s. The results obtained in terms of speed, volume, and distribution coincide largely with those reported for the Popocatépetl volcano gorges (Caballero and Capra 2014; Haddad et al. 2016; Muñoz-Salinas et al. 2009) and for Colima volcano gorges (Caballero et al. 2016; Capra et al. 2018), as well as with the simulation of the 2012 lahar in the Jamapa Gorge of Pico de Orizaba (Franco-Ramos et al. 2020).

The results and methodology employed in this work have implications in different aspects. The first is associated with the way in which risks from lahars are approached both in Mexico and around the world. Although there are already studies dealing with their behavior and possible scopes are analyzed, there are still gaps such as magnitude, triggers, and reconstructions over long periods of time. All these aspects were considered in this work and that is how the longest reconstructions of laharic flow magnitudes for Mexico and possibly in the world was obtained. Another implication of this work is related to the elaboration of hazard maps for Pico de Orizaba volcano, as the information generated may be useful to update existing maps. Also, it is important to highlight that the methods used in the research can be replicated in tropical areas where active volcanoes are subject to the impact of hurricanes.

We conclude that the use of new technologies such as UAVs, photogrammetry, 2D modelling, and tree-ring evidences in a sector of Jamapa Gorge was a useful and accurate method to date natural phenomena such as lahars. For the study area, 8 lahar events were identified in 1931, 1960, 1968, 1975, 1999, 2012, 2014, and 2016. The lahars of 1975 and 2012 had the greatest distribution and number of affected trees. Their formation was mainly associated with torrential rainfalls resulting from the passage of hurricanes and tropical storms. This research represents a contribution to the study of hydrogeomorphic processes on volcanic terrains in central Mexico by providing discharge reconstructions for a period of almost 100 years, as well as the direct association between the formation of lahars and their triggers. The methods can be applied in other gorges of Pico de Orizaba as well as in other volcanoes with similar conditions.

Author contribution
Not applicable.

Declarations

Competing interests   The authors declare no competing interests.

References

Baker VR (2008) Paleoflood hydrology: origin, progress, prospects. Geomorphology 101:1–13. https://doi.org/10.1016/j.geomorph.2008.05.016

Ballesteros Cánovas JA, Eguibar M, Bodoque JM, Díez-Herrero A, Stoffel M, Gutiérrez-Pérez I (2011) Estimating flash flood discharge in an ungauged mountain catchment with 2D hydraulic models and dendrogeomorphic palaeostage indicators. Hydrol Process 25:970–979. https://doi.org/10.1002/hyp.7888

Ballesteros JA, Bodoque JM, Díez-Herrero A, Sanchez-Silva M, Stoffel M (2011) Calibration of floodplain roughness and estimation of flood discharge based on tree-ring evidence and hydraulic modelling. J Hydrol 403:103–115. https://doi.org/10.1016/j.jhydrol.2011.03.045

Ballesteros-Cánovas JA, Stoffel M, Spyt B, Janecka K, Kaczka RJ, Lempa M (2016) Paleoflood discharge reconstruction in Tatra Mountain streams. Geomorphology 272:92–101. https://doi.org/10.1016/j.geomorph.2015.12.004

Benito G, Thorndycraft VR (2005) Palaeoflood hydrology and its role in applied hydrological sciences. J Hydrol 313:3–15. https://doi.org/10.1016/j.jhydrol.2005.02.002

Bodoque JM, Díez-Herrero A, Eguibar MA, Benito G, Ruiz-Villanueva V, Ballesteros-Cánovas JA (2015) Challenges in paleoflood hydrology applied to risk analysis in mountainous watersheds - a review. J Hydrol 529:449–467. https://doi.org/10.1016/j.jhydrol.2014.12.004

Bollschweiler M, Stoffel M, Vázquez-Selem L, Palacios D (2010) Tree-ring reconstruction of past lahar activity at Popocatépetl volcano, Mexico. Holocene 20:265–274. https://doi.org/10.1177/0959683609350394

Bono L, Amigo Á (2015) Modelamiento de los lahares ocurridos en el volcán Calbuco 2015 con el software RAMMS. XIV Congr Geológico Chil:162–165

Bühler Y, Christen M, Kowalski J, Bartelt P (2011) Sensitivity of snow avalanche simulations to digital elevation model quality and resolution. Ann Glaciol 52:72–80. https://doi.org/10.3189/172756411797252121

Caballero L, Capra L (2014) The use of FLO2D numerical code in lahar hazard evaluation at Popocatépetl volcano: A 2001 lahar scenario. Nat Hazards Earth Syst Sci 14:3345–3355. https://doi.org/10.5194/nhess-14-3345-2014

Caballero L, Capra L, Vázquez R, Riley K, Webley P, Thompson M (2016) Evaluating the performance of FLO2D for simulating past lahar events at the most active Mexican volcanoes: Popocatépetl and Volcán de Colima. Natural Hazard Uncertainty Assessment: Modeling and Decision Support; Geophys Monograph: Washington, DC, USA, 223:179-189

Cannon SH, Reneau SL (2000) Conditions for generation of fire-related debris flows, Capulin Canyon, New Mexico. Earth Surf Process Landf 25:1103–1121

Capra L, Borselli L, Varley N, Gavilanes-Ruiz JC, Norini G, Sarocchi D, Caballero L, Cortes A (2010) Rainfall-triggered lahars at Volcán de Colima, Mexico: Surface hydro-repellency as initiation process. J Volcanol Geotherm Res 189:105–117. https://doi.org/10.1016/j.jvolgeores.2009.10.014

Capra L, Coviello V, Borselli L, Márquez-Ramírez VH, Arámbula-Mendoza R (2018) Hydrological control of large hurricane-induced lahars: evidence from rainfall-runoff modeling, seismic and video monitoring. Nat Hazards Earth Syst Sci 18:781–794. https://doi.org/10.5194/nhess-18-781-2018

Carrasco-Núñez G (2000) Structure and proximal stratigraphy of Citlaltépetl volcano (Pico de Orizaba), Mexico. Spec Pap Geol Soc Am 334:247–262. https://doi.org/10.1130/0-8137-2334-5.247

Carrasco-Núñez G, Díaz-Castellón R, Siebert L, Hubbard B, Sheridan MF, Rodríguez SR (2006) Multiple edifice-collapse events in the Eastern Mexican Volcanic Belt: the role of sloping substrate and implications for hazard assessment. J Volcanol Geotherm Res 158:151–176. https://doi.org/10.1016/j.jvolgeores.2006.04.025

Charbonnier SJ, Gertisser R (2012) Evaluation of geophysical mass flow models using the 2006 block-and-ash flows of Merapi Volcano, Java, Indonesia: towards a short-term hazard assessment tool. J Volcanol Geotherm Res 231–232:87–108. https://doi.org/10.1016/j.jvolgeores.2012.02.015

Chiarle M, Iannotti S, Mortara G, Deline P (2007) Recent debris flow occurrences associated with glaciers in the Alps. Glob Planet Chang 56:123–136. https://doi.org/10.1016/j.gloplacha.2006.07.003

Chmutina K, Von Meding J, Bosher L (2019) Language matters: dangers of the "natural disaster" misnomer. Glob Aasessment Rep disaster risk Reduct 2019:1–22

Christen M, Bühler Y, Bartelt P, et al (2012) Integral hazard management using a unified software environment. In: 12th Congress Interpraevent (pp. 77–86)

Comisión Nacional del Agua (CONAGUA) (2014) Caracterización fluvial e hidráulica de las inundaciones en México.

Davila N, Capra L, Gavilanes-Ruiz JC, Varley N, Norini G, Vazquez AG (2007) Recent lahars at Volcán de Colima (Mexico): drainage variation and spectral classification. J Volcanol Geotherm Res 165:127–141. https://doi.org/10.1016/j.jvolgeores.2007.05.016

Díaz V, Paredes C, García C et al (2010) Árboles Longevos De México. Rev Mex Ciencias For 1:7–29

Díez-Herrero A, Ballesteros-Cánovas JA, Bodoque JM, Ruiz-Villanueva V (2013a) A new methodological protocol for the use of dendrogeomorphological data in flood risk analysis. Hydrol Res 44:234–247. https://doi.org/10.2166/nh.2012.154

Díez-Herrero A, Ballesteros JA, Ruiz-Villanueva V, Bodoque JM (2013b) A review of dendrogeomorphological research applied to flood risk analysis in Spain. Geomorphology 196:211–220. https://doi.org/10.1016/j.geomorph.2012.11.028

ESRI (2016) ArcGIS Desktop: Release 10.5.

Fernández de Castro Martínez G, Vázquez Selem L, Palacio Prieto JL, et al (2018) Geomorfometría y cálculo de erosión hídrica en diferentes litologías a través de fotogrametría digital con drones. Investig Geográficas https://doi.org/10.14350/rig.59548

Fischer J-T, Kowalski J, Pudasaini SP (2012) Topographic curvature effects in applied avalanche modeling. Cold Reg Sci Technol 74–75:21–30. https://doi.org/10.1016/j.coldregions.2012.01.005

Franco-Ramos O, Stoffel M, Vázquez-Selem L, Capra L (2013) Spatio-temporal reconstruction of lahars on the southern slopes of Colima volcano, Mexico – a dendrogeomorphic approach. J Volcanol Geotherm Res 267:30–38. https://doi.org/10.1016/j.jvolgeores.2013.09.011

Franco-Ramos O, Castillo M, Muñoz-Salinas E (2016a) Using tree-ring analysis to evaluate intra-eruptive lahar activity in the Nexpayantla Gorge, Popocatépetl volcano (central Mexico). Catena 147:205–215. https://doi.org/10.1016/j.catena.2016.06.045

Franco-Ramos O, Stoffel M, Vázquez-Selem L (2016b) Tree-ring based record of intra-eruptive lahar activity: Axaltzintle valley, Malinche volcano, Mexico. Geochronometria 43:74–83. https://doi.org/10.1515/geochr-2015-0033

Franco-Ramos O, Stoffel M, Vázquez-Selem L (2017) Tree-ring based reconstruction of rockfalls at Cofre de Perote volcano, Mexico. Geomorphology 290:142–152. https://doi.org/10.1016/j.geomorph.2017.04.003

Franco-Ramos O, Stoffel M, Ballesteros-Cánovas JA (2019) Reconstruction of debris-flow activity in a temperate mountain forest catchment of central Mexico. J Mt Sci 16:2096–2109. https://doi.org/10.1007/s11629-019-5496-6

Franco-Ramos O, Ballesteros-Cánovas JA, Figueroa-García JE, Vázquez-Selem L, Stoffel M, Caballero L (2020) Modelling the 2012 lahar in a sector of Jamapa Gorge (Pico de Orizaba Volcano, Mexico) using RAMMS and tree-ring evidence. Water 12:333. https://doi.org/10.3390/w12020333

Garrote J, Díez-Herrero A, Génova M et al (2018) Improving flood maps in ungauged fluvial basins with dendrogeomorphological data. An Example from the Caldera de Taburiente National Park (Canary Islands, Spain). Geosciences 8:300. https://doi.org/10.3390/geosciences8080300

Haddad B, Palacios D, Pastor M, Zamorano JJ (2016) Smoothed particle hydrodynamic modeling of volcanic debris flows: application to Huiloac Gorge lahars (Popocatépetl volcano, Mexico). J Volcanol Geotherm Res 324:73–87. https://doi.org/10.1016/j.jvolgeores.2016.05.016

Holmes RL (1983) Computer-assisted quality control in tree-ring dating and measurement. Tree-Ring Bull 43:69–78

Hoskuldsson A, Robin C (1993) Late Pleistocene to Holocene eruptive activity of Pico de Orizaba, Eastern Mexico. Bull Volcanol 55:571–587. https://doi.org/10.1007/BF00301810

Iverson RM, Schilling SP, Vallance JW (1998) Objective delineation of lahar-inundation hazard zones. Geol Soc Am Bull 110:972–984

Lugo-Hubp J (1988) Elementos de geomorfología aplicada, 1era Edici. Universidad Nacional Autónoma de México, Mexico

Luna Q (2007) Assessment and modelling of two lahars caused by "Hurricane Stan" at Atitlan, Guatemala, October 2005 (Master's thesis)

Morales Martínez MA, Welsh Rodríguez CM, Ruelas Monjardín LC et al (2016) Afectaciones por posible asociación de eventos hidrometeorológicos y geológicos en los municipios de Calcahualco y Coscomatepec, Veracruz. Teoría y Prax 12:31–49. https://doi.org/10.22403/UQROOMX/TYPNE2016/02

Muñoz-Salinas E, Castillo-Rodríguez M, Manea V, Manea M, Palacios D (2009) Lahar flow simulations using LAHARZ program: Application for the Popocatépetl volcano, Mexico. J Volcanol Geotherm Res 182:13–22. https://doi.org/10.1016/j.jvolgeores.2009.01.030

National Oceanic and Atmospheric Administration (NOAA) (2019) Historical Hurricanes Tracks. https://coast.noaa.gov/hurricanes/. Accessed 1 Dec 2019

Nocentini M, Tofani V, Gigli G, Fidolini F, Casagli N (2015) Modeling debris flows in volcanic terrains for hazard mapping: the case study of Ischia Island (Italy). Landslides 12:831–846. https://doi.org/10.1007/s10346-014-0524-7

O'Brien JS, Julien PY, Fullerton WT (1993) Two-dimensional water flood and mudflow simulation. J Hydraul Eng 119:244–261. https://doi.org/10.1061/(ASCE)0733-9429(1993)119:2(244)

Pierson TC, Major JJ (2014) Hydrogeomorphic effects of explosive volcanic eruptions on drainage basins. Annu Rev Earth Planet Sci 42:469–507. https://doi.org/10.1146/annurev-earth-060313-054913

Pierson TC, Pringle PT, Cameron KA (2011) Magnitude and timing of downstream channel aggradation and degradation in response to a dome-building eruption at Mount Hood, Oregon. Bull Geol Soc Am 123:3–20. https://doi.org/10.1130/B30127.1

Pierson TC, Wood NJ, Driedger CL (2014) Reducing risk from lahar hazards: concepts, case studies, and roles for scientists. J Appl Volcanol 3:1–25. https://doi.org/10.1186/s13617-014-0016-4

Prado-Lallande A (2017) Geomorfología, dendrocronología y análisis sedimentológico en la cuenca alta del valle Alcalican, SW del volcán Iztaccíhuatl. Tesis de Licenciatura, Universidad Nacional Autónoma de México

Quesada-Román A, Ballesteros-Cánovas JA, Granados-Bolaños S, Birkel C, Stoffel M (2020) Dendrogeomorphic reconstruction of floods in a dynamic tropical river. Geomorphology 359:107133. https://doi.org/10.1016/j.geomorph.2020.107133

Rinn F (2003) TSAP-Win. Time series analysis and presentation for dendrochronology and related applications. 22

Robinson WJ, Evans R (1980) A microcomputer-based tree-ring measuring system. Tree-Ring Bull 40:59–64

Rodríguez SR, Mora-González I, Murrieta-Hernández JL (2006) Flujos de baja concentración asociados con lluvias de intensidad extraordinaria en el flanco sur del volcán Pico de Orizaba (Citlaltépetl), México. Bol Soc Geol Mex 58:223–236. https://doi.org/10.18268/bsgm2006v58n2a5

Salaorni E, Stoffel M, Tutubalina O, Chernomorets S, Seynova I, Sorg A (2017) Dendrogeomorphic reconstruction of lahar activity and triggers: Shiveluch volcano,

Kamchatka Peninsula, Russia. Bull Volcanol 79. https://doi.org/10.1007/s00445-016-1094-4

Schilling S (2014) Laharz_py: GIS tools for automated mapping of lahar inundation hazard zones. US Department of the Interior, Geological Survey

Servicio Meteorológico Nacional (SMN) (2008) https://smn.cna.gob.mx. Accessed 28 Nov 2019

Servicio Meteorológico Nacional (SMN) (2012) https://smn.cna.gob.mx. Accessed 28 Nov 2019

Servicio Meteorológico Nacional (SMN) (2016) https://smn.cna.gob.mx. Accessed 28 Nov 2019

Siebe C, Abrams M, Sheridan MF (1993) Major Holocene block-and-ash fan at the western slope of ice-capped Pico de Orizaba volcano, México: implications for future hazards. J Volcanol Geotherm Res 59:1–33. https://doi.org/10.1016/0377-0273(93)90075-3

Smith GA, Fritz WJ (1989) Volcanic influences on terrestrial sedimentation. Geology 17:375

Staley DM, Kean JW, Cannon SH, Schmidt KM, Laber JL (2013) Objective definition of rainfall intensity-duration thresholds for the initiation of post-fire debris flows in southern California. Landslides 10:547–562. https://doi.org/10.1007/s10346-012-0341-9

Stevens N, Manville V, Heron D (2003) The sensitivity of a volcanic flow model to digital elevation model accuracy: experiments with digitised map contours and interferometric SAR at Ruapehu and Taranaki volcanoes, New Zealand. J Volcanol Geotherm Res 119:89–105. https://doi.org/10.1016/S0377-0273(02)00307-4

Stoffel M, Corona C (2014) Dendroecological dating of geomorphic disturbance in trees. Tree-Ring Res 70:3–20. https://doi.org/10.3959/1536-1098-70.1.3

Stoffel M, Bollschweiler M, Vázquez-Selem L, Franco-Ramos O, Palacios D (2011) Dendrogeomorphic dating of rockfalls on low-latitude, high-elevation slopes: Rodadero, Iztaccíhuatl volcano, Mexico. Earth Surf Process Landf 36:1209–1217. https://doi.org/10.1002/esp.2146

Stokes MA, Smiley TL (1968) An introduction to tree–ring dating. University of Chicago Press, Chicago, IL

Thouret JC, Antoine S, Magill C, Ollier C (2020) Lahars and debris flows: characteristics and impacts. Earth-Science Rev 201:103003. https://doi.org/10.1016/j.earscirev.2019.103003

Tichavský R, Koutroulis A, Chalupová O, Chalupa V, Šilhán K (2020) Flash flood reconstruction in the Eastern Mediterranean: regional tree ring-based chronology and assessment of climate triggers on the island of Crete. J Arid Environ 177:104135. https://doi.org/10.1016/j.jaridenv.2020.104135

UN (2015) Sendai Framework for Disaster Risk Reduction 2015–2030. http://www.unisdr.org/files/43291_sendaiframeworkfordrren.pdf. Accessed 18 Jan 2021

Vargas G, Rutllant J, Ortlieb L (2006) ENSO tropical–extratropical climate teleconnections and mechanisms for Holocene debris flows along the hyperarid coast of western South America (17°–24°S). Earth Planet Sci Lett 249:467–483. https://doi.org/10.1016/j.epsl.2006.07.022

Vàzquez R, Capra L, Caballero L et al (2014) The anatomy of a lahar: deciphering the 15th September 2012 lahar at Volcán de Colima, Mexico. J Volcanol Geotherm Res 272:126–136. https://doi.org/10.1016/j.jvolgeores.2013.11.013

Voellmy A (1955) Über die Zerstörungskraft von Lawinen. Schweiz Bauztg 73:159–162

Wilhelm B, Ballesteros Cánovas JA, Macdonald N, Toonen WHJ, Baker V, Barriendos M, Benito G, Brauer A, Corella JP, Denniston R, Glaser R, Ionita M, Kahle M, Liu T, Luetscher M, Macklin M, Mudelsee M, Munoz S, Schulte L, St. George S, Stoffel M, Wetter O (2019) Interpreting historical, botanical, and geological evidence to aid preparations for future floods. Wiley Interdiscip Rev Water 6:e1318. https://doi.org/10.1002/wat2.1318

Williams R, Stinton AJ, Sheridan MF (2008) Evaluation of the Titan2D two-phase flow model using an actual event: case study of the 2005 Vazcún Valley Lahar. J Volcanol Geotherm Res 177:760–766. https://doi.org/10.1016/j.jvolgeores.2008.01.045

Worni R, Huggel C, Stoffel M, Pulgarín B (2012) Challenges of modeling current very large lahars at Nevado del Huila Volcano, Colombia. Bull Volcanol 74:309–324. https://doi.org/10.1007/s00445-011-0522-8

J. E. Figueroa-García (✉)
Posgrado en Geografía,
Universidad Nacional Autónoma de México, Ciudad Universitaria Coyoacán,
Ciudad de México, 04510, México
Email: ernestfigue.7@gmail.com

J. A. Ballesteros-Cánovas
Institute of Environmental Science,
University of Geneva,
Carl-Vogt 66, CH-1205, Geneva, Switzerland

O. Franco-Ramos · L. Vázquez-Selem
Instituto de Geografía,
Universidad Nacional Autónoma de México, Ciudad Universitaria,
04510, Coyoacán, Ciudad de México, México

J. M. Bodoque
Department of Mining and Geological Engineering,
University of Castilla-La Mancha,
Avda. Carlos III, 45071, Toledo, Spain